UNCLASSIFIED

~~SECRET~~

UCRL-2706

Classified Physics and Mathematics

UNIVERSITY OF CALIFORNIA

Radiation Laboratory
Berkeley, California

Contract No. W-7405-eng-48

AEC RESEARCH AND DEVELOPMENT REPORT

NEUTRON PRODUCTION BY HIGH-ENERGY PARTICLES

Walter E. Crandall and George P. Millburn

September 29, 1954

Photostat Charge $ 4.59 for
Access Permittees

Available from
Technical Information Service
P. O. Box 1001, Oak Ridge, Tennessee

Printed for the U. S. Atomic Energy Commission

~~SECRET~~ UNCLASSIFIED

NEUTRON PRODUCTION BY HIGH-ENERGY PARTICLES

Walter E. Crandall and George P. Millburn

Radiation Laboratory, Department of Physics
University of California, Berkeley, California

September 29, 1954

ABSTRACT

From neutron-yield measurements made with a $MnSO_4$ detecting solution, the average number of neutrons produced per inelastic event is determined for a series of elements from lithium to uranium for 340-Mev protons, 190-and 315-Mev deuterons, 490-Mev He^3 ions, and 90-and 160-Mev neutrons. The results are analyzed in an attempt to understand the total yield measurements for thick targets and to explain the variation of yield with the atomic number of the target.

***

I. INTRODUCTION

In attempting to explain the yield of neutrons from targets bombarded by high-energy particles,[1] information concerning the number of neutrons produced per inelastic event, $\bar{N}$, and the cross section for the production of one neutron, σ_{1N}, is needed. These two quantities have been determined for a variety of elements for 340-Mev protons, 90-Mev neutrons, 160-Mev neutrons, 190-Mev deuterons, 320-Mev deuterons, and 490-Mev He^3 particles.

The measurements were made by detecting the neutrons in a tank of $MnSO_4$ solution.[1] The targets were equal to or less than the range of the charged particles in most cases.

Inelastic cross sections for the various particles were taken from

California Research and Development Co. Report LRL-85, by Birnbaum et al. (see also Phys. Rev. 95, 1268 (1954)).

In general the values of $\bar{N}$ and ϵ_{1N} increase rapidly with increasing atomic weight, whereas the increase with particle energy is much slower.

II. MEASUREMENTS

1. Neutron Yields

The number of neutrons emitted from a target, N_n, for P_n incident particles was measured in a $MnSO_4$ solution contained in a large tank.[1] Eighteen inches of solution surrounded the 1-foot-square tunnel in which the targets were placed. The plug at the rear of the tunnel was removed when the targets were less than a range thick, and for all targets in the neutron beams. The solution was calibrated by placing a calibrated neutron source (Ra-Be) in the tunnel. The activity induced in the manganese was counted by two sets of thin-walled Geiger counters. For further details concerning the method, UCRL-2063 should be consulted. The relative error in measurement is estimated to be 3 percent, but because of the uncertainty in the neutron source calibration, the absolute error is about 10 percent.

2. Beam Monitors

The number of charged particles incident on the target was measured by a parallel-plate ionization chamber operated so as to render negligible the effects of recombination.[1] The ionization chamber was calibrated against a Faraday cup. The charges collected were determined by measuring the voltage produced across a calibrated condenser with a 100-percent inverse feedback electrometer. The condensers were calibrated against a "secondary standard" condenser, which was calibrated by the National Bureau of Standards to 0.1 per cent. For further details, UCRL-2063 should be consulted. The relative error in measurement is estimated to be 1 percent, and the absolute error about 2 percent, or less.

The neutron beams used in this experiment were monitored by a scintillation counter telescope using the recoil protons from a CH_2 target and the measured n-p differential cross sections. The monitor was "calibrated" by counting CH_2, C, and no targets. The relative error is estimated to be less than 1 percent, but the absolute error is about 10 percent, mainly because of the uncertainty in the n-p cross section. A more complete description of the telescope and its use will appear in a UCRL report by Whitehead and others concerning measurements of the energy distribution of the 160 Mev neutron beam and the measurement of $C^{12}(n,2n)C^{11}$ cross sections.

3. Particles

The charged particles used which could be accelerated directly in the 184-inch synchrocyclotron (340-Mev protons, 190-Mev deuterons, and 490-Mev He^3 particles) were very monoergic beams. In addition, deuterons of approximately 320 Mev were produced by stripping He^3 particles in an internal target.[2] ~~This~~ beam had an energy spread of about 60 Mev at half maximum with a low-energy tail.[2]

The neutron beams used were produced by stripping 190-Mev deuterons and 490 Mev He^3 particles in a 1/2-inch carbon target. The mean energies were 90 and 160 Mev, with energy spreads at half maxima of about 20 and 50 Mev respectively. Measurements could not be made with the 270-Mev neutron beam produced by 340-Mev protons because of the low intensity of the beam.

4. Targets

The targets used included elements from lithium to uranium, but not all targets were used for all the above particles. In Table I we list the targets used for the various particles. Some of the data used in the calculations were three or four years old, and the thicknesses of these targets were known only in inches. The densities given in the Handbook of Chemistry and Physics, 34th Edition, 1952-1953, were used in such cases. Except for the 5/8-by-4-1/4-inch diameter, 2 x 2-and 3 x 3-inch targets, all uranium targets were of milled square bars of either 6 or 12 inches in length. The density of the bars was 18.6 g/cm^3. One lithium target was contained in a stainless steel cylinder with 0.010-inch stainless steel windows on either end; a recent recalculation of the range of 190-Mev deuterons in lithium showed that this target was only half the range in thickness. Since the plug of $MnSO_4$ (18 inches thick) at the end of the tank tunnel[1] was not removed during bombardment, the measured value of N/P_2 is certainly too high because of further neutron production by deuterons in the plug. The measured value was corrected for the deuteron production in the $MnSO_4$ plug, and more recently another lithium target was used.

5. Errors

The accuracy of the measurements will be discussed in terms of comparison of relative values for different targets and different beams. The absolute values may be in error by a further 10 percent because of inaccuracies in the neutron-source calibration. Corrections for possible systematic errors were not applied except as noted.

The values of N/P_n for the directly accelerated charged particle beams have a standard error of about 4 percent on a relative basis. The values of the yield for the 320-Mev deuterons have a standard error of about 6 percent, with an additional uncertainty in interpreting the results because of the energy distribution of the beam. The error in N/P_n for the neutron beams is due almost entirely to the error in the n-p cross section and is about 10 percent. To compare the neutron data at the two energies, a relative error of about 3 percent may be used.

The combined errors in the cross section and the target thickness were estimated to be about 10 percent (i.e., the error in σt was assumed to be 10 percent).

The errors in the quantities $\overline{N}$ and σ_{1N} were calculated by the method of propagation of errors. The error in σ_{1N} due to an error in σt tends to cancel for thin targets with the result that σ_{1N} is generally more accurate than $\overline{N}$.

III. CALCULATIONS

1. Definitions

The average number of neutrons emitted during an inelastic event may be defined as

$$\overline{N} = \frac{\eta}{1 - e^{-\sigma_n t}} , \qquad (1)$$

where $\eta = N/P_n$ corrected for background and secondary particle production, t is the thickness of the target, and σ_n is the inelastic cross section for a bombarding particle of n nucleons. The cross section for the production of one neutron may then be defined as

$$\sigma_{1N} = \sigma_n \overline{N} = \frac{\eta \sigma_n}{1 - e^{-\sigma_n t}} . \qquad (2)$$

For small values of t this reduces to $\sigma_{1N} = \eta/t$, which shows clearly that errors in σ_n tend to cancel in calculating σ_{1N}.

On the assumption that the nucleons in a multi-nucleon particle are independent at these high energies, the number of inelastic events for a particle with n nucleons may be taken as $n(1 - e^{-\sigma_1 t})$, in which case

$$\overline{N}' = \frac{\eta}{n(1 - e^{-\sigma_n t})} , \tag{3}$$

and taking $\sigma_{1N'} = \sigma_1 \overline{N}_1$,

$$\sigma_{1N'} = \frac{\eta \sigma_1}{n(1 - e^{-\sigma_1 t})} . \tag{4}$$

These values of $\sigma_{1N'}$ and $\overline{N'}$ are calculated as well as those defined in Eqs. (1) and (2), and are referred to as the cross section per nucleon and average number of neutrons per inelastic event per nucleon.

2. Background

The yield for no target, $(N/P_n)_o$, was measured for all beams used. When the neutron beams were used, the neutrons passed through the tunnel in the $MnSO_4$ tank and did not impinge on any concentration of material near the tank. Thus the yield is taken as

$$\frac{N}{P_n} - \left(\frac{N}{P_n}\right)_o$$

for the neutron beams.

When the charged-particle beams pass through the tunnel, the particles hit the back wall of the experimental enclosure[1] and produce neutrons which may then be detected by the tank. The "background" measured in this way may be compared with the "background" measured with an absorber of slightly more than one range inserted in the far end of the 40-inch collimator;[1] for 340-Mev protons the yield in the first case is 20 times greater than in the second case; for 190-Mev deuterons, the ratio is about 5, but in this case the relatively high yield of stripped neutrons in the forward direction causes the measurement to be only an upper limit for the true background.

Thus the measured $(N/P_n)_o$ can not be used directly as the background when charged-particle beams are used. Instead, the background was calculated by assuming

The yield of neutrons varies about as the square of the particle energy,[1]

The "true" background is zero,

The range of charged particles varies about as the square of the particle energy.

Then the yield should vary about as the range of the particles, and the background for targets less than a range in thickness is

$$\left(\frac{N}{P_n}\right)_{Bgd} = \left(\frac{N}{P_n}\right)_o \frac{R_o - t}{R_o} e^{-\sigma_n t}, \qquad (5)$$

where R_o is the range of the particle. The background was less than 20 percent of the measured yield (see Table II).

5. Secondary Effects

For thick targets the high-energy particles produced in the target may undergo inelastic collisions and produce further neutrons. To correct for this effect, it is necessary to know the number, kind, and energies of the secondary particles and the average number of neutrons produced per secondary collision. The corrections should be small and apply only to the high-energy particles produced. In the case of uranium, low-energy neutrons may cause further production by inducing fission; no attempt has been made to correct for this effect. Further, absorption of neutrons in the target has been neglected.

For deuterons incident on the targets, the secondary production was calculated only for the stripped neutrons produced. The known stripping cross sections, σ_{2s}, were used and the $\bar{N}$ measured for 90-Mev neutrons was used. The secondary production is then

$$\int_0^t \sigma_1 \bar{N}\, dx \int_0^x e^{-\sigma_2 x}\, \sigma_{2s}\, e^{-\sigma(x-\lambda)}\, d\lambda,$$

and since $\sigma_{2sp} = \sigma_2 - \sigma_1$, the integrations give

$$\bar{N}[(1 - e^{-\sigma_1 t}) - \frac{\sigma_1}{\sigma_2}(1 - e^{-\sigma_2 t})]. \qquad (6)$$

The corrections varied from zero for thin targets to 5 percent for a range thickness of uranium, the highest correction found. The correction is only a lower limit, but under the assumptions made above is certainly good to within a factor of 2. If a reasonable value of $\bar{N}$ is used for 90-Mev protons, the correction for stripped proton production is negligible.

For the 90-Mev neutron beam the secondary production of the cascade neutrons produced has been calculated by assuming[3]

(a) The cascade neutrons are emitted isotropically in the forward hemisphere only,

(b) The mean effective energy for production of the cascade neutrons is about 50 to 60 Mev, giving an average of $\bar{N} = 8$ neutrons per inelastic collision,

(c) The mean number of cascade neutrons produced per inelastic collision is $c = 0.86$.

The production due to the fast effect and the absorption of neutrons has again been neglected, as has the production caused by the cascade protons produced in the target. Then the secondary production $\overline{N}_s$ is given by

$$\overline{N}_s = \sigma_1^2 c\overline{N} \int_0^t dx \int_0^x f_x \, e^{-\sigma_1 \lambda} \, e^{-\sigma_1 \sqrt{(x-\lambda)^2 + a^2}} \, d\lambda \,, \tag{7}$$

where

$$f_x = \frac{2}{\pi} \tan^{-1} \frac{b}{(x - \lambda)\sqrt{(x - \lambda)^2 + c^2}} \tag{8}$$

is the solid-angle[4] effect due to the assumed angular distribution, and a, b, c are geometrical constants of the target.

For the 160-Mev neutron data, $c\overline{N}$ was taken equal to 10.

4. Data and Results

The data used in this report are presented in Table II. The standard errors listed are those assigned from statistical variations of the data from several determinations, plus the errors listed in Sec. II5. No corrections were applied except as listed in the previous sections, and errors due to uncertainties in the applied corrections and neglected secondary effects were not included in the final error assigned, except in the case of Li(1) and Be.

The calculated values of $\overline{N}$ and σ_{1N} defined according to Eqs. (1) and (2) are listed in Table III and plotted in Figs. 1 and 3. The values of $\overline{N}'$ and $\sigma_{1N'}$ calculated from the definitions of Eqs. (3) and (4) are listed in Table IV. $\overline{N}'$ is plotted in Fig. 2 as a function of mean nucleon energy.

Previously, B. B. Kinsey[5] measured the number of neutrons produced per inelastic collision for 90-Mev neutrons. His results are shown in Fig. 1 for comparison. No measurements of the inelastic cross sections existed at the time of his work, and he used 0.36 of the measured total cross sections for σ_1. The small difference between the two values for uranium is completely removed upon recalculating Kinsey's data with our value of σ_1. The factor-of-two difference in $\bar{N}$ for the medium-weight elements cannot be explained by the differences in the inelastic cross sections used in the two experiments.

IV. ANALYSIS OF RESULTS

The yield of neutrons from a target bombarded by charged particles may be expressed

$$\eta = \int_0^t \sigma_{1N} \, e^{-\sigma_n x} \, dx \qquad (9)$$

if secondary events are neglected. In terms of the energy, Eq. (9) is

$$\eta = \int_{E_0}^{E} \sigma_{1N} \, e^{-\sigma_n x} \frac{1}{dE/dx} \, dE , \qquad (10)$$

so that the quantity $\sigma_{1N}(dE/dx)^{-1}$ gives a quick estimate of the manner in which the yield will vary with energy for different particles. If the stopping power, dE/dx, is expressed in the units Mev (g/cm^2)$^{-1}$, then (dE/dx)(A/A_0), where A is the mass number of the element and A_0 is Avogadro's number, is the stopping power in units of Mev (nuclei /cm^2)$^{-1}$. The quantity $[\sigma_{1N}/(dE/dx)][A_0/A]$ is listed in Table IV and plotted in Fig. 4. The steep rise in the curve, which begins near A = 230, is probably caused by the onset of fission; if the 2.5 neutrons per fission are subtracted from $\bar{N}$ for 190-Mev deuterons on uranium, the value of $[\sigma_{1N}/(dE/dx)][A_o/A]$ drops from 0.0248 to 0.0177; the latter value falls near a smooth curve through the other points. The anomolous behavior of the lithium and beryllium points is probably a reflection of the small number of particles in these nuclei and the fact that the predominant isotopes of these nuclei have one extra neutron.

It is important to note that since the stopping power decreases by almost a factor of two between carbon and uranium, the relative productivity of different elements is given more realistically in Fig. 4 than in Fig. 3.

The secondary processes in the targets may be important, particularly if the primary target is one range thick and backed by a uranium target. If the particles are deuterons, the total production in the primary target is given by

$$y = \int_0^R \sigma_{1N}(d) e^{-\sigma_2 x}\, dx + \int_0^R \sigma_{1N}(n)\, dx \int_0^x e^{-\sigma_2 \lambda}\, \sigma_{2s}\, e^{-\sigma_1 (x-\lambda)}\, d\lambda \qquad (11)$$

if the secondary production by stripped neutrons only is considered; here $\sigma_{1N}(d)$ is the cross section for deuterons and $\sigma_{1N}(n)$ is the cross section for neutrons of approximately half the deuteron energy. For a primary target backed by uranium of thickness t, the additional production is given by

$$y_s = \int_0^t \sigma_{1N}(n)\, e^{-\sigma_1 \lambda}\, d\lambda \int_0^R e^{-\sigma_2 x}\, \sigma_{2s}\, e^{-\sigma_1 (R-x)}\, dx, \qquad (12)$$

so the total production is

$$Y = y + y_s = \bar{N}(d)(1 - e^{-\sigma_2 R}) + \bar{N}(n)[(1 - e^{-\sigma_1 R}) - (\sigma_1/\sigma_2)(1 - e^{-\sigma_2 R})]$$

$$+ \bar{N}(n)e^{-\sigma_1 R}(1 - e^{-\sigma_{2s} R})(1 - e^{-\sigma_1 t}). \qquad (13)$$

This expression neglects the angular distribution of the stripped neutrons, the secondary charged particles and knock-on neutrons (important for low-A elements), and the high-energy secondary particles produced in the second target. Its general form agrees with the empirical formula[1] from the external yield data. Table V lists the calculated and observed[1] yields for a one-range target with $t = 0$ and $t = \infty$. The assumed values of $\bar{N}$ were taken from Fig. 2 to correspond to deuterons of 130 and 210 Mev energies. The general agreement for 190 Mev is probably fortuitous. The discrepancy for one range of beryllium may be due in part to multiplication of the stripped neutrons in the $MnSO_4$ plug at the rear of the tank; the corrected value ($\eta = 0.74 \pm 0.17$) listed in Table II is probably a better estimate of y_{obs} and agrees with $y_{calc} = 0.65$.

As is evident from Eqs. (12) and (13), an estimate of the neutron production in the secondary target is best given in terms of $\sigma_{2s}/(dE/dx)$ for deuterons. This is listed in Table VI. In order to compare the expected total yield as a function of the target material, the ratios $\sigma_{2s}/(dE/dx)$ should be multiplied by $\bar{N}(n)$, and since the secondary target is usually uranium, $\bar{N}(n)$ for uranium should be used. These numbers are given in Table VI together with the sum

$$\frac{\sigma_{2s}}{dE/dx}\bar{N}(n) + \frac{\sigma_{1N}}{dE/dx}.$$

The various ratios of the calculated and observed values are given in Table VIII. The calculated values $[\sigma_{2s}/(dE/dx)]\bar{N}(n)$, $[\sigma_{1N}/(dE/dx)]$, and their sum are plotted as a function of the mass number of the primary target in Fig. 5.

The figure clearly shows that a target should be selected from either the heavy or the light elements. The calculated superiority of the light elements shown in Fig. 5 is not found experimentally as shown in Table VIII; the discrepancy may be due to the neglect of attenuation of the stripped neutrons (greatest in the light elements), or, more likely, may be due to the naivete of the calculations.

V. ACKNOWLEDGMENTS

This work was done under the general supervision of Dr. C. M. Van Atta and with the assistance of F. Adelman, W. Birnbaum, D. Hicks, J. Ise, Jr., R. Main, R. Pyle, L.Schecter and M. Whitehead. Similar measurements were first inaugurated by Prof. E. O. Lawrence and were further developed by Prof. H. York and others. All the measurements reported here were made at the 184-inch synchrocyclotron at Berkeley, except for the 230-Mev deuteron data, which were measured at the Institute for Nuclear Studies at the University of Chicago.

This work was performed under the auspices of the U. S. Atomic Energy Commission.

Table I

Description of Basic Target Dimensions

Designation	Description (inches)	Density (g/cm^3)
Uranium U(1)	4-1/4 dia. cylinder	18.6
U(2)	1/16 and 1/8 x 2 x 2 squares	
U(3)	1/16 x 3 x 3 squares	
U(4)	1/2 x 1/2 x 6 bars (milled)	
U(5)	1 x 1 x 6 bars (milled)	
U(6)	1-1/8 x 1-1/8 x 12 bars (milled)	
U(7)	1/2 x 1/2 x 12 bars (milled)	
Thorium	4-1/4 dia. cylinder	11.3
Lead		11.35
Cadmium		8.65
Molybdenum	4 x 4 squares	10.2
Copper		8.94
Aluminum		2.70
Carbon		1.8
Beryllium	4-1/4 dia. cylinder	1.95
Lithium (1)	2 x 2 squares (see pg. 4)	0.534
Lithium (2)	4 dia. cylinder	

Table II

Data and Results

Target	Thickness	$\frac{N}{F_n}$	$\frac{N}{F_n}$ Bgd	η	$\bar{N}$	σ_{1N}	$\bar{N}'$	$\sigma_{1N'}$	$\bar{E}$ Mev
A. 190-Mev Deuteron Beam									
U(2)	1/16 in.	0.332	0.066	0.266 ± 0.005	9.5 ± 1.0	36.2 ± 0.70	8.8 ± 0.9	17.9 ± 0.3	187
	1/8 in.	0.560	0.057	0.491 ± 0.011	8.9 ± 0.8	33.9 ± 0.8	8.2 ± 0.9	16.6 ± 0.4	180
	1/4 in.	1.08	0.040	1.01 ± 0.01	9.4 ± 0.9	35.8 ± 0.4	8.6 ± 0.9	17.5 ± 0.2	170
	1/2 in.	1.93	0.012	1.87 ± 0.02	9.1 ± 0.7	34.6 ± 0.4	8.2 ± 0.8	16.6 ± 0.2	140
	5/8 in.	2.30	0	2.20 ± 0.0[illegible]	8.9 ± 1.1	33.9 ± 1.2	7.8 ± 0.9	15.8 ± 0.6	130
U(1)	5/8 in.	2.35	0	2.25 ± 0.1[illegible]	8.9 ± 1.0	33.9 ± 2.3	7.8 ± 1.3	15.8 ± 1.2	130
	5/8 in.	2.34	0	2.24 ± 0.[illegible]7	9.0 ± 0.9	34.3 ± 1.1	7.9 ± 1.0	16.0 ± 0.5	130
U(3)	12.07 g/cm^2	1.04	0.02	1.01 ± 0.05	9.2 ± 1.2	35.0 ± 1.7	8.4 ± 1.2	17.1 ± 0.9	170
Th	1.0 in.	2.14	0	2.05 ± 0.07	8.4 ± 0.9	31.7 ± 1.0	7.4 ± 0.9	14.8 ± 0.5	130
	14.82 g/cm^2	1.12	0.02	1.08 ± 0.08	8.0 ± 0.9	30.2 ± 2.2	7.3 ± 1.3	14.6 ± 1.1	160
	14.87 g/cm^2	1.15	0.03	1.10 ± 0.04	8.1 ± 0.8	30.8 ± 1.1	7.4 ± 0.9	14.8 ± 0.5	160
Pb	12.39 g/cm^2	0.756	0.032	0.713 ± 0.030	6.1 ± 0.6	21.0 ± 0.9	5.6 ± 0.6	10.2 ± 0.4	160
Cd	12.24 g/cm^2	0.622	0.020	0.585 ± 0.020	4.01 ± 0.30	9.6 ± 0.3	3.6 ± 0.4	4.5 ± 0.2	160
Mo	1.0 in.	1.01	0	0.98 ± 0.10	3.4 ± 0.3	7.5 ± 0.8	3.1 ± 0.7		130
Cu	11.48 g/cm^2	0.426	0.024	0.395 ± 0.018	2.30 ± 0.24	4.05 ± 0.19	2.3 ± 0.3	1.94 ± 0.09	160
	11.74 g/cm^2	0.428	0.017	0.403 ± 0.020	2.26 ± 0.21	3.98 ± 0.20	2.2 ± 0.3	1.9 ± 0.1	160
	1.0 in	0.78	0	0.75 ± 0.08	2.4 ± 0.3	4.2 ± 0.4	2.3 ± 0.5	2.0 ± 0.2	130
Al	11.92 g/cm^2	0.306	0.015	0.286 ± 0.015	1.22 ± 0.09	1.22 ± 0.06	1.2 ± 0.2	0.56 ± 0.04	150
	2-3/4 in.	0.46	0	0.45 ± 0.05	1.3 ± 0.2	1.3 ± 0.1	1.3 ± 0.3	0.61 ± 0.06	130

MU-8373

Table II

Data and Results (Cont.)

Target	Thickness	$\frac{N}{F_n}$	$\frac{N}{F_n}$ Bgd	η	$\bar{N}$	σ_{1N}	$\bar{N}'$	$\sigma_{1N'}$	$\bar{E}$ Mev
A. 190-Mev Deuteron Beam (Cont.)									
C	7.67 g/cm^2	0.187	0.023	0.158 ± 0.014	0.70 ± 0.09	0.47 ± 0.04	0.88 ± 0.09	0.215 ± 0.019	160
Be	10.20 g/cm^2	0.455	0.017	0.427 ± 0.015	1.45 ± 0.12	0.73 ± 0.03	1.8 ± 0.1	0.333 ± 0.012	160
	4 in.	0.91	0	0.74 ± 0.12	1.7 ± 0.3	0.88 ± 0.15	2.0 ± 0.3	0.37 ± 0.06	130
Li(2)	4-1/2 in.	0.238	0.030	0.194 ± 0.012	0.89 ± 0.10	0.41 ± 0.03	1.0 ± 0.1	0.170 ± 0.011	170
Li(1)	6 in.	0.71	?	0.42 ± 0.15	1.5 ± 0.4	0.70 ± 0.25	1.9 ± 0.7	0.32 ± 0.11	160
B. [illegible]-Mev Deuteron Beam									
U(1)	1.0 in.	3.25	0	3.00 ± 0.15	8.2 ± 0.8	31.2 ± 1.6	7.0 ± 1.0	14.0 ± 0.7	150
C. [illegible]-Mev Deuteron Beam									
U(7)	1/2 in.	2.28	0.12	2.0[illegible] ± 0.10	10.2 ± 1.0	38.8 ± 1.9	9.2 ± 1.3	18.4 ± 0.9	300
	1.0 in.	4.55	0.05	4.21 ± 0.15	11.5 ± 1.0	43.8 ± 1.8	9.7 ± 1.2	19.4 ± 0.7	270
D. 490-Mev He^3 Ion Beam									
Cd	6.10 g/cm^2	0.413	0.063	0.350 ± 0.04	4.2 ± 0.6	11.2 ± 1.1	3.0 ± 1.1	3.6 ± 0.4	450
	12.24 g/cm^2	0.752	0.038	0.714 ± 0.07	4.5 ± 0.6	11.8 ± 1.2	3.1 ± 1.0	3.8 ± 0.4	400
Ta	28.8 g/cm^2	1.80	0	1.8 ± 0.2	6.5 ± 0.9	23.4 ± 2.3	4.2 ± 1.5	7.2 ± 0.7	315
U	54.15 g/cm^2	3.26	0	3.0 ± 0.3	11.0 ± 1.4	48.4 ± 4.8	7.4 ± 2.3	15.9 ± 1.6	315

MU-8374

Table II

Data and Results (Cont.)

Target	Thickness	$\frac{N}{P_n}$	$\frac{N}{P_n}$ Bgd	η	$\bar{N}$	σ_{1N}	$\bar{E}$ Mev
E. <u>340-Mev Proton Beam</u>							
U(1)	2-5/8 in.	7.30	0	7.30 ± 0.30	16.0 ± 1.3	29.6 ± 1.2	220
U(3)	62.35 g/cm^2	4.42	0.041	4.38 ± 0.19	17.4 ± 1.7	32.2 ± 1.4	280
	94.4 g/cm^2	6.48	0.08	6.40 ± 0.11	17.6 ± 1.4	33.4 ± 0.7	250
	47.2 g/cm^2	3.95	0.24	3.71 ± 0.08	18.3 ± 1.7	34.8 ± 0.7	300
	23.6 g/cm^2	2.17	0.38	1.79 ± 0.07	16.7 ± 1.7	31.8 ± 1.2	320
Th	32.45 g/cm^2	1.97	0.068	1.90 ± 0.10	13.3 ± 1.4	24.4 ± 1.3	320
	62.14 g/cm^2	3.87	0.041	3.83 ± 0.24	15.0 ± 1.6	27.4 ± 1.7	300
Cd	30.71 g/cm^2	1.17	0.063	1.11 ± 0.04	6.85 ± 0.68	7.33 ± 0.26	300
	61.43 g/cm^2	1.94	0.031	1.91 ± 0.10	6.44 ± 0.64	6.89 ± 0.36	270
Cu	29.93 g/cm^2	0.690	0.059	0.631 ± 0.040	3.41 ± 0.37	2.46 ± 0.16	300
	59.82 g/cm^2	1.20	0.026	1.17 ± 0.04	3.50 ± 0.30	2.52 ± 0.09	270
Al	28.8 g/cm^2	0.381	0.053	0.328 ± 0.040	1.48 ± 0.22	0.58 ± 0.07	300
	57.5 g/cm^2	0.684	0.018	0.666 ± 0.042	1.69 ± 0.17	0.66 ± 0.04	260

MU-8375

Table II

Data and Results (Cont.)

Target	Thickness	$\frac{N}{P_n}$	$\frac{N}{P_n}$ Bgd	η	$\bar{N}$	σ_{1N}
F. <u>90-Mev Neutron Beam</u>						
U(4)	1/2 in.	1.4	0.013	1.4 ± 0.4	12.4 ± 3.8	25 ± 8
	1/2 in.	1.26	0.03	1.23 ± 0.12	10.9 ± 1.5	21.8 ± 0.7
	1 in.	2.36	0.03	2.33 ± 0.24	11.0 ± 1.5	22.0 ± 0.8
U(5)	1 in.	2.46	0.03	2.37 ± 0.25	11.1 ± 1.5	22.2 ± 2.2
U(6)	1-1/8 in.	2.80	0.03	2.68 ± 0.28	11.4 ± 1.6	22.8 ± 0.4
	3-3/8 in.	7.35	0.03	6.84 ± 0 [illegible]	12.4 ± 1.6	24.8 ± 0.4
	6-3/4 in.	10.7	0.03	9.8 ± 1.[illegible]	12.2 ± 1.4	24.4 ± 0.3
	10-1/8 in.	12.2	0.03	11.1 ± 1.2	12.2 ± 1.4	24.4 ± 0.4
	14-5/8 in.	12.7	0.03	11.4 ± 1.3	11.8 ± 1.3	23.6 ± 0.8
Cd	1-3/8 in.	0.47	0.013	0.46 ± 0.05	2.6 ± 0.3	3.1 ± 0.3
Cu	2-5/8 in.	0.86	0.013	0.85 ± 0.09	2.2 ± 0.3	1.9 ± 0.2
	1-5/16 in.	0.426	0.013	0.41 ± 0.04	1.9 ± 0.3	1.6 ± 0.2
Al	4-1/4 in.	0.252	0.013	0.24 ± 0.02	0.91 ± 0.11	0.43 ± 0.04
C	6-13/16 in.	0.303	0.013	0.29 ± 0.03	0.92 ± 0.12	0.22 ± 0.02
G. <u>160-Mev Neutron Beam</u>						
U(6)	2-1/4 in.	6.6	0.4	5.8 ± 0.04	14.2 ± 1.4	28 ± 3
	5 in.	11.2	0.4	9.6 ± 1.1	13.9 ± 1.8	27 ± 3
	9 in.	16.4	0.4	13.7 ± 1.6	15.6 ± 1.9	30 ± 3
	15-3/4 in.	17.9	0.4	14.7 ± 1.8	15.1 ± 1.8	29 ± 3

MU-8376

Table III

Average Values of $\bar{N}$, σ_{1N}, $\bar{N}'$ and $\sigma_{1N'}$

Element	Particle	Incident Energy (Mev)	$\bar{N}$	σ_{1N}	$\bar{N}'$	$\sigma_{1N'}$
Uranium	Deuteron	190	9.1 ± 0.3	34.9 ± 0.9	8.2 ± 0.4	16.7 ± 0.8
		230	8.2 ± 0.8	31.2 ± 1.6	7.0 ± 1.0	14.0 ± 0.7
		320	10.8 ± 1.0	41.3 ± 2.5	9.4 ± 1.2	18.9 ± 0.7
	Proton	340	17.2 ± 0.8	33.0 ± 1.4		
	He^3 Ion	490	11.0 ± 1.4	48.4 ± 4.8	7.4 ± 2.3	15.9 ± 1.6
	Neutron	90	11.0 ± 1.5	22.0 ± 2.5		
		160	14 ± 2	27 ± 3		
Thorium	Deuteron	190	8.1 ± 0.8	30.5 ± 1.0	2.4 ± 1.0	14.8 ± 0.5
	Proton	340	14.1 ± 1.2	25.9 ± 2.2		
Lead	Deuteron	190	6.1 ± 0.6	21.0 ± 0.9	5.6 ± 0.6	10.2 ± 0.4
Tantalum	He^3 Ion	490	6.5 ± 0.9	23 ± 2	4.2 ± 1.5	7.2 ± 0.7
Cadmium	Deuteron	190	4.01 ± 0.30	9.6 ± 0.3	3.6 ± 0.4	4.5 ± 0.2
	Proton	340	6.65 ± 0.6	7.1 ± 0.3		
	He^3 Ion	490	4.4 ± 0.6	11.5 ± 1.0	3.0 ± 1.0	3.7 ± 0.4
	Neutron	90	2.6 ± 0.4	3.1 ± 0.3		
Copper	Deuteron	190	2.28 ± 0.20	4.02 ± 0.20	2.3 ± 0.3	1.94 0.09
	Proton	340	3.5 ± 0.3	2.49 ± 0.08		
	Neutron	90	2.0 ± 0.3	1.7 ± 0.2		
Aluminum	Deuteron	190	1.22 ± 0.01	1.22 ± 0.06	1.2 ± 0.2	0.58 ± 0.04
	Proton	340	1.59 ± 0.15	0.62 ± 0.04		
	Neutron	90	0.91 ± 0.15	0.43 ± 0.04		
Carbon	Deuteron	190	0.70 ± 0.0[illegible]	0.47 ± 0.04	0.88 ± 0.09	0.215 ± 0.019
	Neutron	90	0.92 ± 0.15	0.22 ± 0.02		
Beryllium	Deuteron	190	1.45 ± 0.12	0.73 ± 0.03	1.8 ± 0.1	0.333 ± 0.012
Lithium	Deuteron	190	0.89 ± 0.10	0.41 ± 0.03	1.0 ± 0.1	0.170 ± 0.011

MU-8377

Table IV

Ratio of σ_{1N} to Stopping Power of Charged Particles

Element	190-Mev deuterons	340-Mev protons	320-Mev deuterons
Uranium	0.0248	0.0509	0.0417
Thorium	0.0222	0.0408	
Lead	0.0168		
Cadmium	0.0116	0.0192	
Copper	0.00746	0.0105	
Aluminum	0.00455	0.0054	
Carbon	0.0034		
Beryllium	0.0076		
Lithium	0.0055		

Table V

Calculated and Observed External Neutron Yields for Deuterons

Target	$\bar{N}(d)$	$\bar{N}(n)$	y_{calc} (t=0)	y_{obs} (t=0)	t (in.)	Y_{calc} (t=∞)	Y_{obs} (t=∞)
A. 190-Mev Deuterons							
Uranium	9.1	9.0	2.38	2.34 ± 0.07		3.35	3.32
Thorium	8.1	7.8	2.15	2.14 ± 0.06		3.16	2.95
Copper	2.28	1.6	0.72	0.78 ± 0.08		2.02	1.90
Aluminum	1.22	[illegible].7	0.42	0.46 ± 0.05		1.88	1.90
Carbon	0.70	0.7	0.30	---		2.38	2.3
Beryllium	1.45	0.7	0.65	0.91 ± 0.09(?)		2.88	2.90
B. 320-Mev Deuterons							
Uranium	10.8	16	6.2	(6.7 ± 0.2)	8-1/2	11.1	9.43 ± 0.3
Carbon	0.83	1.3	0.76	1.2 ± 0.2	10-1/8	7.5	4.3 ± 0.2
Beryllium	1.72	1.3	1.5	1.9 ± 0.2	8-1/2	7.9	---

Table VI

Ratio of Stripping Cross Section to Rate of Energy Loss for Deuterons

Element	σ_{2s} (barns)	190-Mev deuterons $\sigma_{2s}/(dE/dx)$	320-Mev deuterons $\sigma_{2s}/(dE/dx)$
Uranium	1.78	0.00127	0.00274
Thorium	1.76	0.00128	
Lead	1.63	0.00130	
Cadmium	1.16	0.00140	
Copper	0.91	0.00172	
Aluminum	0.53	0.00197	
Carbon	0.42	0.00306	
Beryllium	0.32	0.00332	
Lithium	0.30	0.00402	

Table VII

Ratio of Stripping Cross Section to Stopping Power of 190-Mev Deuterons Multiplied by $\bar{N}(n)$ for Uranium

Element	$\frac{\sigma_{2s}}{dE/dx}\bar{N}(n)$	$\frac{\sigma_{1N}}{dE/dx} + \frac{\sigma_{2s}}{dE/dx}\bar{N}(n)$
Uranium	0.0140	0.0388
Thorium	0.0141	0.0363
Lead	0.0143	0.0311
Cadmium	0.0154	0.0280
Copper	0.0189	0.0264
Aluminum	0.0217	0.0263
Carbon	0.0337	0.0371
Beryllium	0.0366	0.0442
Lithium	0.0443	0.0498

Table VIII

Calculated and Observed Ratios of Yields for 190-Mev Deuterons

Element	$\frac{\sigma_{1N}}{dE/dx}$	Observed Primary Target Yield	$\frac{\sigma_{2s}}{dE/dx}$	Observed Secondary Target Yield	Sum	Observed Total External Yield
Uranium	1.000	1.000	1.00	1.00	1.000	1.000
Thorium	0.895	0.915	1.01	0.85	0.935	0.89
Lead	0.676	---	1.02	--	0.801	--
Cadmium	0.468	---	1.10	--	0.721	--
Copper	0.301	0.334	1.35	1.35	0.680	0.57
Aluminum	0.183	0.196	1.55	1.69	0.677	0.45
Carbon	0.137	---	2.41	--	0.955	0.57
Beryllium	0.306	0.389	2.62	2.02	1.140	0.87
Lithium	0.222	?	3.16	?	1.283	?

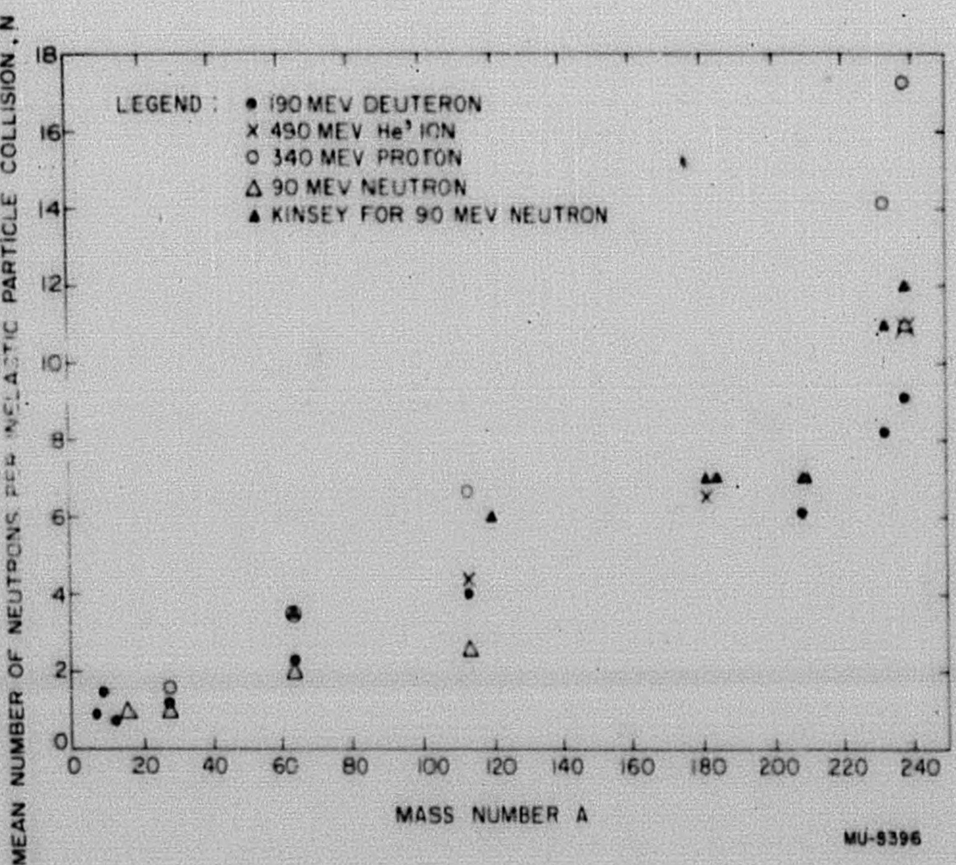

Figure 1

The mean number of neutrons produced per inelastic collision of an incident particle as given by Eq. (1) of the text vs. mass number A of the target. The values of $\overline{N}$ for 90-Mev neutrons from this report and Kinsey's experiment are not directly comparable because different inelastic cross sections were used; correcting his cross section for uranium brings his value down to 11 but does not remove the discrepancy at copper and the apparent discrepancy near A = 110.

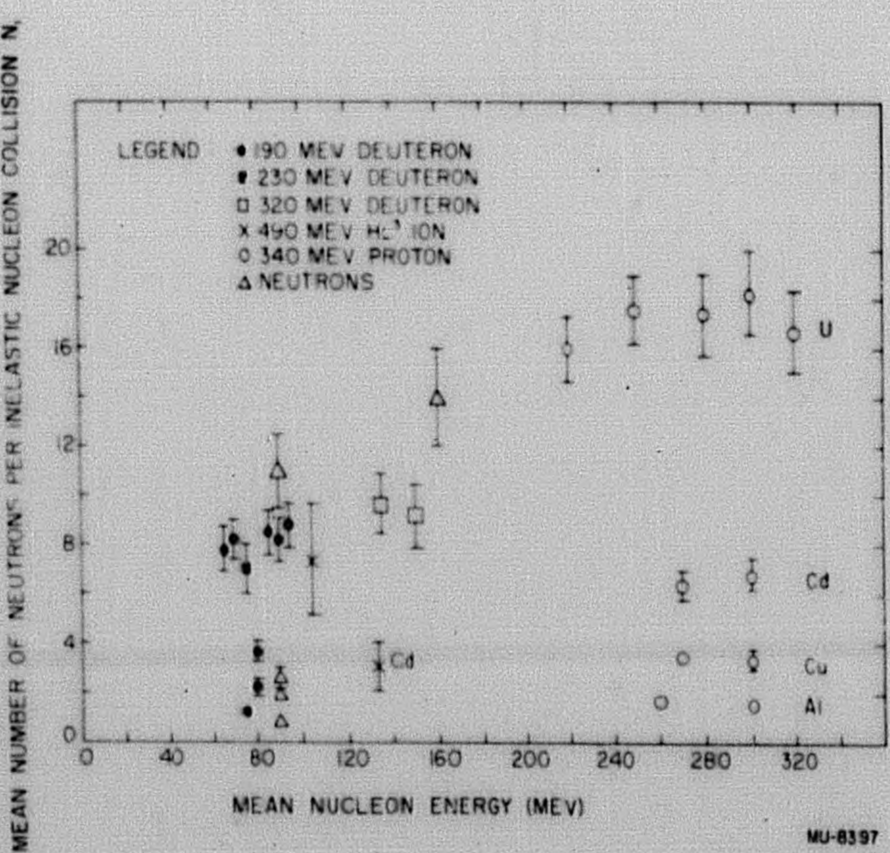

Figure 2

The mean number of neutrons produced per inelastic collision of an incident nucleon as given by Eq. (3) of the text vs. mean nucleon energy. Points are shown for uranium, cadmium, copper and aluminum targets. The mean energy was taken to be the energy of the nucleon (particle energy divided by number of nucleons in the particle) at the middle of the target. The variation of energy for the same particle is the result of using targets of different thicknesses. The data for the low-A elements from 90-Mev neutrons appear to be systematically low as compared with the trend for uranium.

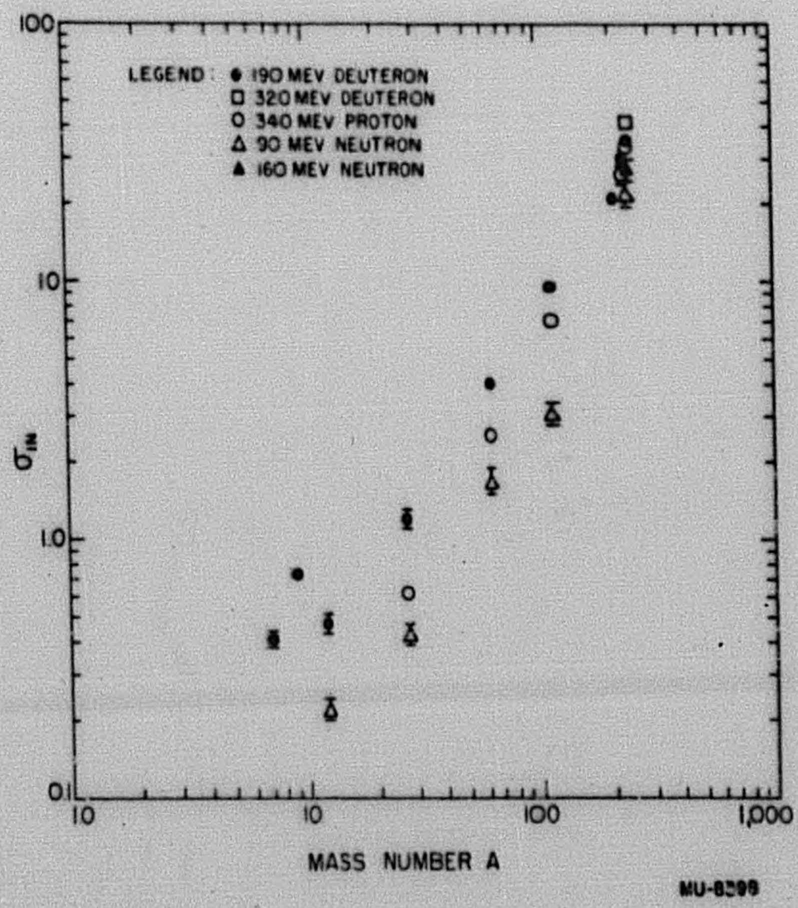

Figure 3

The cross section for producing one neutron as given by Eq. (2) of the text vs. mass number A of the target.

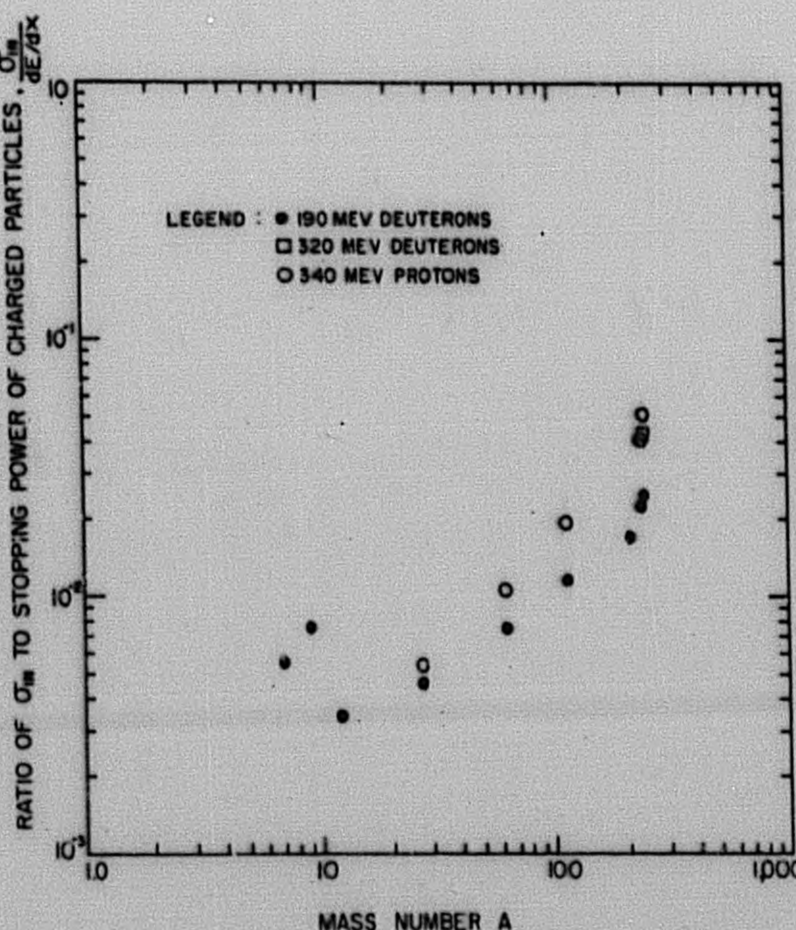

MU-6399

Figure 4

The ratio of σ_{1N} to stopping power per atom for charged particles as a function of the target mass number. The points should be roughly proportional to the neutron yield from targets of one range or less thickness.

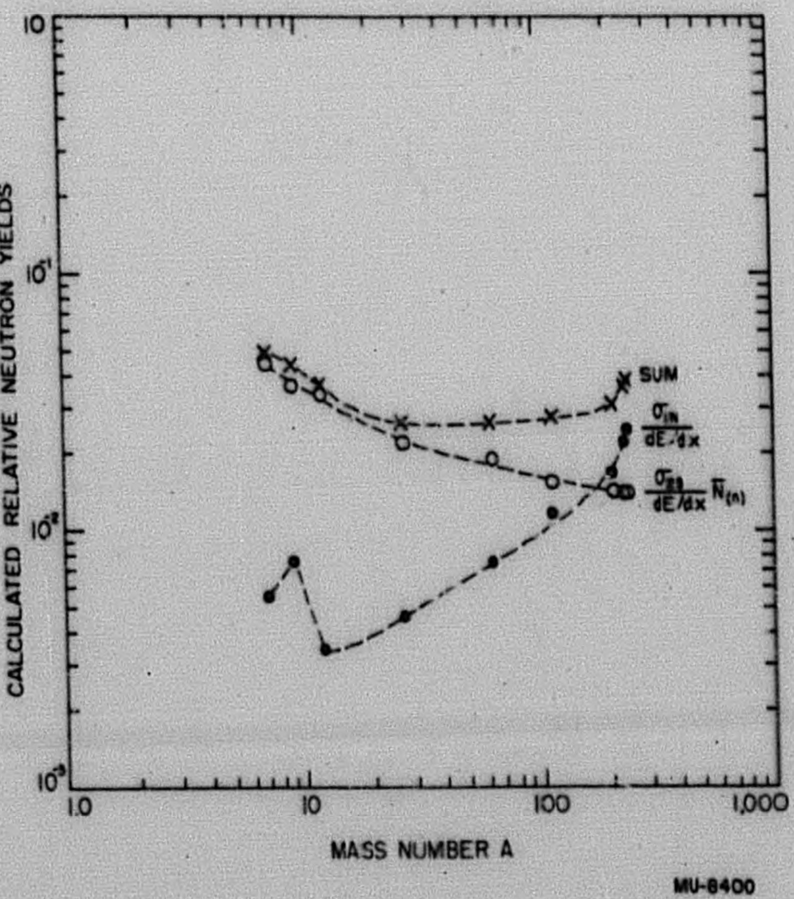

Figure 5

The quantities [$\sigma_{1N}/(dE/dx)$], [$\sigma_{2s}/(dE/dx)$] $\bar{N}$ (n), and their sum for 190-Mev deuterons as a function of the target mass number. The solid dots are $\sigma_{1N}/(dE/dx)$ and should be roughly proportional to the yield from targets up to one range thick; the open dots are [$\sigma_{2s}/(dE/dx)$] $\bar{N}$(n) (where $\bar{N}$(n) is the average number of neutrons produced when a 60-Mev neutron has an inelastic event in uranium) and should be roughly proportional to the yield from a primary target of mass number A backed by a thick uranium secondary target. For comparison with observed results, see Table VIII.

REFERENCES

1. W. E. Crandall and G. P. Millburn, Total Neutron Yield from Targets Bombarded by Deuterons and Protons, University of California Radiation Laboratory Report No. UCRL-2063.

2. J. Ise, Jr., R. Pyle, D. Hicks, and R. Main, The Production of 320-Mev Deuterons by He^3 Stripping, University of California Radiation Laboratory Report No. UCRL-2319 (2nd rev.); see also Rev. Sci. Instr. 25, 437 (1954).

3. We are indebted to Prof. E. O. Lawrence, who supplied copies of Monte Carlo calculations communicated to him by H. Mc Manus and W. Sharp.

4. Frank S. Crawford, Jr., Rev. Sci. Instr. 24, 552 (1953).

5. B.B. Kinsey, unpublished.